





LETTER | FEBRUARY 13 2023

The multi-lobed rotation of droplets induced by interfacial reactions

Zhan-Long Wang (王占龙)   ; Kui Lin (林焄)  



Physics of Fluids 35, 021705 (2023)

<https://doi.org/10.1063/5.0137859>



Articles You May Be Interested In

Equilibrium shapes of two- and three-dimensional two-phase rotating fluid drops with surface tension:
Effects of inner drop displacement

Physics of Fluids (November 2022)

Numerical simulation of evolution pattern of vortices in Taylor–Couette flow with three-lobe multiwedge
clearance

Physics of Fluids (June 2024)

Turbulent structures and mixing enhancement with lobed mixers in a supersonic mixing layer

Physics of Fluids (April 2020)



Physics of Fluids

Special Topics Open
for Submissions

[Learn More](#)

The multi-lobed rotation of droplets induced by interfacial reactions

Cite as: Phys. Fluids **35**, 021705 (2023); doi: [10.1063/5.0137859](https://doi.org/10.1063/5.0137859)

Submitted: 6 December 2022 · Accepted: 24 January 2023 ·

Published Online: 13 February 2023



View Online



Export Citation



CrossMark

Zhan-Long Wang (王占龙),^{1,a)} and Kui Lin (林焜),^{2,a)}

AFFILIATIONS

¹Shenzhen Institute of Advanced Technology, Chinese Academy of Sciences, Shenzhen, Guangdong 518000, China

²Department of Civil and Environmental Engineering, The Hong Kong Polytechnic University, Hong Kong, China

^{a)}Authors to whom correspondence should be addressed: zl.wang1@siat.ac.cn and kui-cee.lin@polyu.edu.hk

ABSTRACT

In this Letter, we report a novel phenomenon—that the multi-lobed rotation of a droplet can occur when controlling only its volume and without the use of external devices, which is quite different from previous studies. This phenomenon is based on the interfacial reaction causing the droplet rotation effect. In such a system, the angular velocity and lobe number show an inversely linear relationship with the droplet radius. By controlling the volume of a droplet, we can manipulate it to form four-, three-, and two-lobed shapes. Simple models are also proposed to explain this phenomenon. The results indicate that this phenomenon is consistent with the theory of Scriven and Brown.

Published under an exclusive license by AIP Publishing. <https://doi.org/10.1063/5.0137859>

The rotation and the deformable shapes of droplets are enduring topics of interest and hold great significance in fluids mechanics,^{1–4} nucleonics,⁵ superfluids,^{6–8} and astrophysics.⁹ Droplet rotation also has significant application prospects in devices such as micro/nano-motors, microfluidics chips, and foldable devices.^{10,11} The relevant work on the behavior of a rotating droplet can be tracked back to the experiments carried out by Plateau in 1863.¹² In Plateau's experiments, a droplet was immersed in a density-matched aqueous phase to balance gravity and leave the droplet effectively weightless.^{12,13} The droplet was then rotated, and its deformation was observed. As a simple and effective method, the method that immerses droplets in isopycnic background fluids is still the main way to observe the deformation of droplets until now.^{14,15} However, in such a system, the surrounding fluid exerted a large viscous drag on the rotating droplets, which induced unwanted influences, e.g., the viscous resistance on droplet rotation, unwanted deformation of droplets caused by the surrounding fluid, etc.^{16,17} In this system, the droplets were also difficult to control and spin.

In relevant research studies on droplet rotation and deformation, some effective alternatives were proposed to carry out the experiments of droplet rotation in a simpler, more precise way. Examples included employing magnetic suspension^{18,19} or acoustic levitation^{20–22} to overcome the gravity of a droplet and to further reduce the effect of the surrounding liquid. In related work, Hill and Eaves proposed a method that employs a “liquid electric motor” designed to overcome gravity by diamagnetic levitation and drives droplets to spin by an

applied Lorentz force.^{17,18} However, this research heavily depends on complex or specially designed devices or conditions. Furthermore, in this study, the droplet deformation is realized by controlling the angular velocity of the droplet. Gu *et al.* presented an acoustofluidic centrifugation technique that leverages an entanglement of acoustic wave actuation and the spin of a fluidic droplet to enable nanoparticle enrichment and separation.²⁰ In the above and other similar research studies, the external assistant devices are still indispensable for droplet rotation and deformation observation.

In the ways that get rid of external devices, some researchers have made beneficial attempts and achieved important advances. Pimienta and her coworkers discovered that different water-saturated dichloromethane droplets can form various shapes during rotation on the surface of aqueous solutions of cetyltrimethylammonium bromide (CTAB).^{23,24} Chakrabarti reported that a volatile droplet deposited on a floating swellable sheet can exhibit spontaneous motion including anticlockwise rotation with a star shape.²⁵ However, the volatilization of the droplet results in a shorter rotation life. Recently, studies on the collective motions of active particles^{26,27} and thermal gradients driving droplet rotation^{28,29} have provided novel and promising ways to study droplet rotation and deformation in a simple and spontaneous way. Such research studies generally do not require external devices and remove the influence of the surrounding liquid. These research studies attracted broad interest in the fields of active matter, droplet self-motion, etc. However, there are insurmountable shortcomings in that the angular velocity is difficult to control and, furthermore, it is hard

to make the droplet to deform. Wang *et al.* found that acid droplets can continuously and spontaneously rotate on the surface of liquid metal. However, the multi-lobed shapes during rotation have not been reported.^{30,31} Despite these efforts on the rotation of droplets, finding simple yet effective ways to drive a droplet to rotate with different multi-lobed shapes is still a challenge. In recent years, due to the properties of fission and multi-lobed shapes, droplet rotation, as an effective model in physics, has received much attention in many fields, such as the atomic nucleus, superfluid droplets, and black holes.^{32–34} The search for a non-immersive, simple, and effective driving mode with which to study multi-lobed deformation has been viewed as highly important.

Here, based on previous work on the interfacial reaction causing droplet rotation (IRCDR) effect,^{30,31} we report a novel approach in which a rotating droplet deforms into a multi-lobed shape on the surface of a liquid metal without any external setup. Moreover, the droplet deformation variation is controlled by changing the volume of the droplet, which is quite different from the previous reports that drive the droplet to rotate and produce deformation by controlling angular velocity.^{18,22,35} Compared to other mechanisms of droplet spontaneous rotation, e.g., the collective motion of active particles and thermal gradient, this method has a wider angular velocity range and a more stable rotation state. Moreover, it is also easier to control the deformation and multi-lobed rotation of a droplet by controlling the volume of the droplet. In the experiments, liquid metal and acid droplets are used. The acid droplet is deposited on the surface of a liquid metal. Chemical reactions occur between the droplet and liquid metal. The reactions lead to the dynamic Marangoni force at the contact line, which breaks the asymmetry of the droplet and drives the droplet to rotate under the action of circumferential non-equilibrium Laplace pressure, as reported previously.^{30,31} Under proper conditions, by changing the volume, a rotating droplet can exhibit multi-lobed shapes with two to four lobes. Simple models are proposed to illustrate this phenomenon. Our work offers a novel way to study the multi-lobed shapes of a rotating droplet.

To exhibit this phenomenon, we employed a liquid metal (65% Ga, 35% In, Shenyang Northeast Nonferrous Metals Market Co. Ltd) and dilute sulfuric acid droplets (pH: 0.55, volume V : 0.5–2.5 ml, 98%, Sinopharm Chemical Reagent Co., Ltd, Milli-Q IQ 7000). In the experiments, the oxide film forming on the surface of the liquid metal

had to be scraped off because it could hinder the chemical reaction and pin the contact line, inhibiting the movement of droplets.³⁶ In this system, the droplet is driven to rotate due to interfacial chemical reactions, i.e., the IRCDR effect.^{30,31} In this phenomenon, the droplet boundary begins to oscillate under the surface tension gradient caused by the interfacial chemical reactions. The symmetry of the droplet breaks in this oscillation. The droplet is driven to rotate under the action of circumferential asymmetric Laplace pressure resulting from the curved contact line, as reported in the previous work.^{30,31} This approach that utilizes the IRCDR effect to drive droplets to rotate eliminates the viscous drag effect of the surrounding liquid and gets rid of the external driving devices. The observational apparatus is designed to provide a good view, as shown in Fig. 1(a). The experimental platform consists of a CCD, a droplet injection system, and an optical system. The injection pump controls the droplet volume. The optical system consists of a light source and a beam-splitting prism. The beam-splitting prism is employed to enhance the imaging of the droplet.

Figure 1(b) shows different rotational modes, including two-, three-, and four-lobed shapes, with different droplet volumes. The droplet experiences four-lobed, three-lobed, and two-lobed shapes with increasing volume. The angular velocity Ω decreases from four-lobed to two-lobed shapes. The volume of the droplet dominates the movement patterns under the action of Marangoni instability.³⁷ This is interpreted by considering the wavelength associated with the Marangoni instability and the characteristic length of the droplet.³⁷ In addition, the waves traveling around the droplet equator can drive the droplet to spin, and the small perturbations with different amplitudes lead to varied rotating shapes.¹⁷ On the surface of the liquid metal, an acid droplet reacts with the liquid metal as $2\text{Ga} + 3\text{H}_2\text{SO}_4 = \text{Ga}_2(\text{SO}_4)_3 + 3\text{H}_2\uparrow$. The reactions at the droplet boundary lead to an oscillation of the surface tension gradient at the area near the contact line. With different droplet volumes, this oscillation causes the perturbation of the droplet boundary to different extents. Moreover, during the rotation, the tiny bubbles at the interface can significantly reduce the friction between the droplet and liquid metal, leading to obvious slippage of the droplet according to previously reported work.^{38,39}

Two kinds of multi-lobed droplet shapes, including the pipette-immersed droplet and the free droplet, are shown in detail in Figs. 2

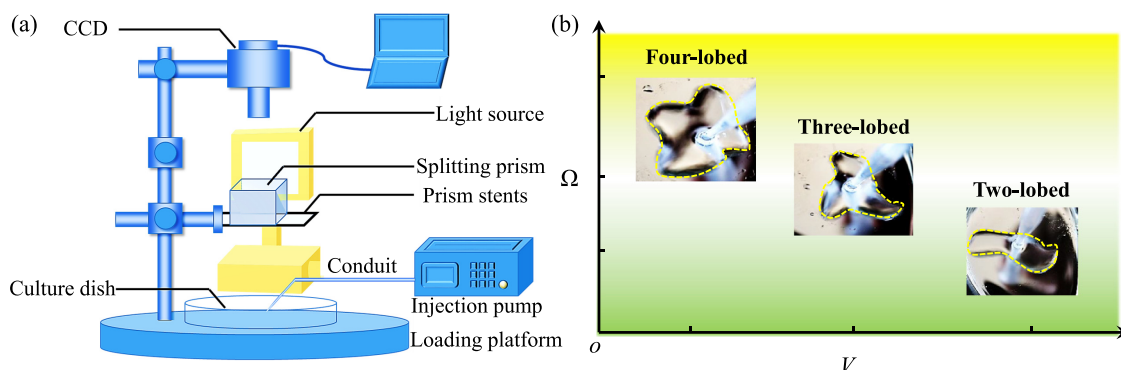


FIG. 1. (a) The experimental equipment used in the experiments. (b) The modes of the multi-lobed rotating shapes of the droplet controlled by V . The shapes change from four- to three- and two-lobed as V increases. The angular velocity decreases with V .

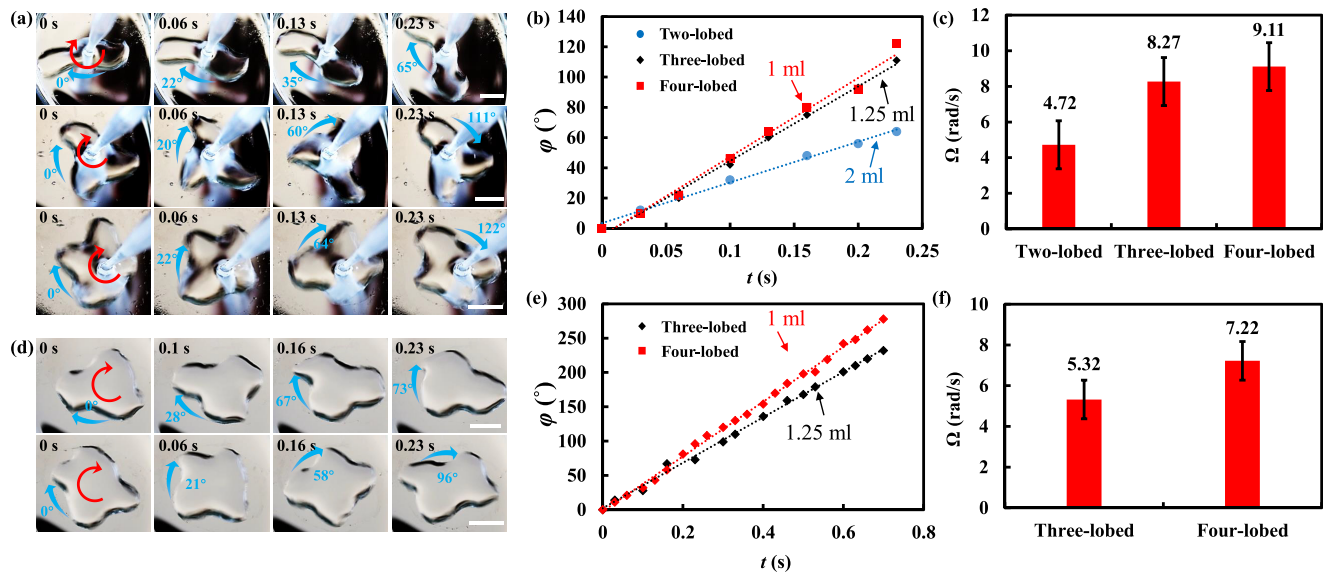


FIG. 2. The multi-lobed shapes and angular velocities Ω of different droplets. (a) Two-, three-, and four-lobed rotations with the pipette immersed in the liquid to constrain the position of the droplet. (b) The RA vs t of the free droplets (V : 1 and 1.25 ml). (c) The comparison of angular velocity in different cases (pipette constraints). Ω decreases with the droplet lobe number, i.e., the droplet shape changes from four-lobed to two-lobed. (d) Three- and four-lobed rotations of a free droplet on liquid metal. (e) The RA of the droplets (V : 1, 1.25, and 2 ml, pipette constraints) vs t , showing a linear relationship that indicates a constant and steady rotation. (f) The angular velocity comparison of the free droplet, which is similar to the cases with the pipette constraint.

and 3. The pipette is immersed in the liquid to constrain the position of the droplet to obtain a stable rotation state. The droplet volumes adopted, corresponding to different shapes for both kinds of deformations, are 1.0 ml (four-lobed), 1.25 ml (three-lobed), and 2 ml (two-lobed), respectively. Figures 2(a) and 3(a) (Multimedia view) show the three shapes of the rotating droplets with a pipette immersed in the liquid. In the upper row, the two-lobed shape is shown. In this situation, the droplet exhibits a shape similar to an “S” and rotates about 56° in 0.2 s. In the middle row, the three-lobed shape is shown. This

droplet is like a three-pronged windmill. In 0.23 s, it rotates about 111° . In the lower row, the four-lobed droplet shape is shown. It is like a *Galium bungei* Steud. It rotates about 122° in 0.23 s. Figure 2(b) show the relationships between the rotation angle ϕ and time t . From the results, ϕ increases linearly with t for all kinds of shapes. This indicates that the droplet rotation is stable and constant. Different slopes indicate varied angular velocities of the rotating droplets. Figure 2(c) shows the angular velocity Ω comparison of different types of rotation. The results show that Ω increases as the lobe number m increases, i.e., as V decreases. Figures 2(d)–2(f) and 3(b) (Multimedia view) show the cases of free droplets. The three-lobed and four-lobed free droplets rotate about 73° and about 96° in 0.23 s, respectively. For free droplets, the oversized volume that is larger than the three-lobed case can lead the droplet to be unstable and prone to split into two individual droplets (supplementary material, Fig. S1). The rotation of the droplet generally lasts tens of seconds. The droplet then tends to come to rest as the concentration of the reactive substance drops below a certain threshold. The long-time, three-lobed rotation of a free droplet, as a typical case, is shown in Fig. 3(c) (Multimedia view).

The deformation degree of the cases in Fig. 2, the relationship between the rotational lobe number m , and the volume V are shown in Fig. 4. The deformable droplet is simplified to the model as shown in Fig. 4(a). The deformation degree is characterized by $W_i = l_i/R_i$ (l_i : the axis length of the droplet lobe; R_i : the initial droplet radius), which represents the comparison between the maximum deformation length and the characteristic length. The dotted line and the dashed-dotted line represent the initial droplet profile and the maximum circumference of the deformation shape, respectively. In Fig. 4(b), the deformation degrees for both cases are shown: $W_{i2} \sim 1.48$, $W_{i3} \sim 1.39$, and $W_{i4} \sim 1.36$ (pipette immersing droplet) and $W_{i3}' \sim 1.24$, $W_{i4}' \sim 1.17$ (free droplet). It can be seen that as V increases, W_i increases and m

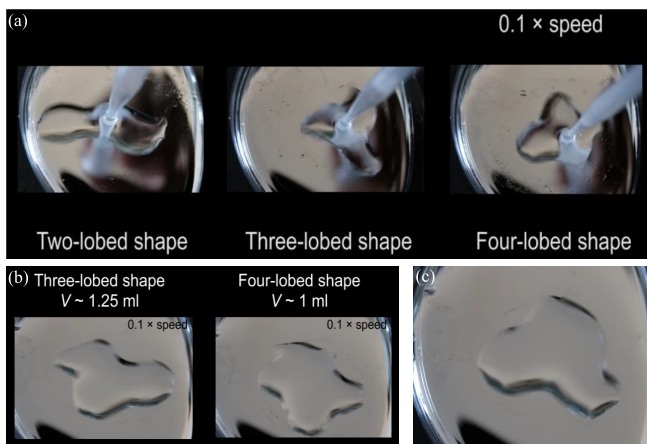


FIG. 3. (a) The multi-lobed shapes of a rotating droplet (pipette immersed case). (b) The multi-lobed shapes of a rotating droplet (free droplet case). (c) The long-time rotation of a rotating droplet with the three-lobed free droplet as an example. Multimedia views: <https://doi.org/10.1063/5.0137859.1>; <https://doi.org/10.1063/5.0137859.2>; <https://doi.org/10.1063/5.0137859.3>

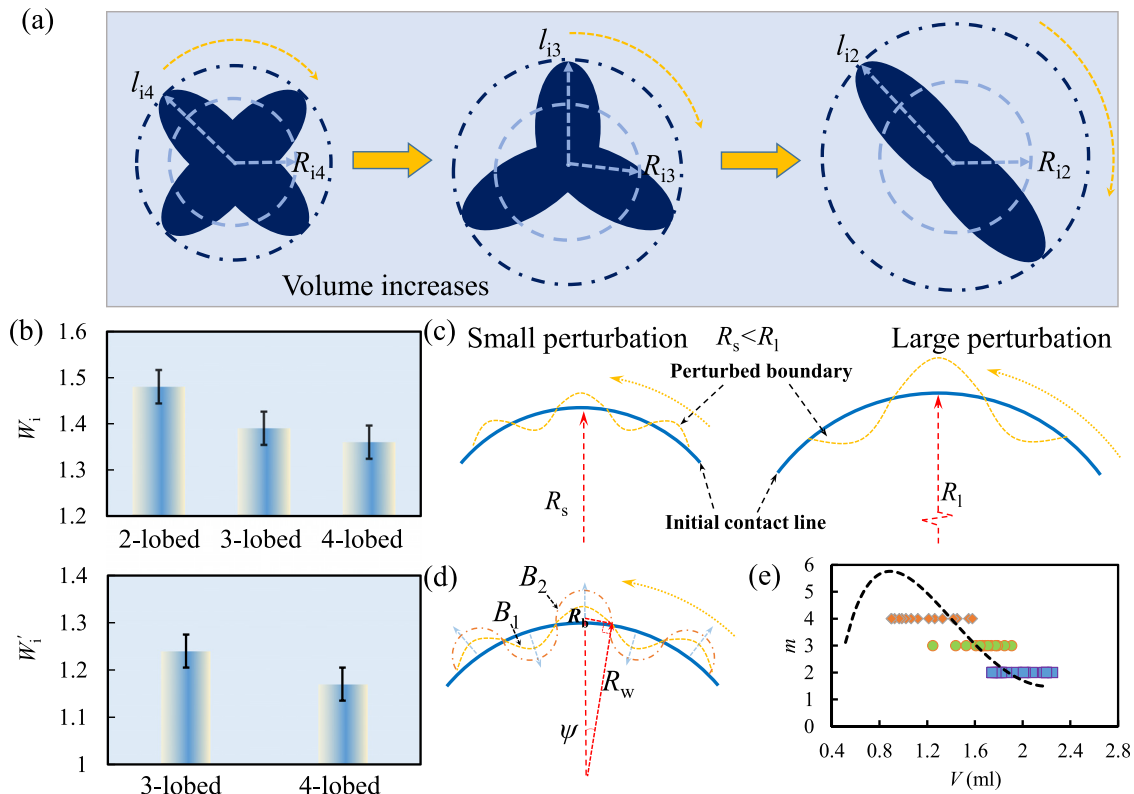


FIG. 4. A diagram of the droplet deformation and the simple analytical model. (a) The simplified model of a droplet after deformation and the parameters characterizing the deformation degree. The dotted line and dash-dotted line represent the initial cycle droplet (radius: R_i) and the maximum circumference of the droplet after deformation (radius: l_i), respectively. (b) The deformation degree W of the multi-lobed shapes of rotating droplets. (c) The diagram of perturbation of the boundary for a small droplet (R_s) and a large droplet (R_l). (d) The analysis model of the droplet lobe number vs the droplet radius. (e) A comparison of the experimental data and an analytical model-fitted curve. The two results show good agreement.

decreases. The rotating droplet shapes and the response of m to V are analyzed with a simplified model. In Fig. 4(c), the droplet boundary deformation of a small droplet (radius R_s) and a large droplet (radius R_l) is illustrated, where $R_s < R_l$. The solid line and dotted line represent the initial contact line and the perturbed boundary, respectively. Chemical reactions at the contact line lead to a surface tension gradient, causing boundary oscillation. According to the previous work on the unified analysis of droplets on a substrate,⁴⁰ we can carry out the following simplified analysis. We can select one point in the contact line of the small and large droplets, respectively. The Laplace pressure at this point can be calculated as $\Delta p = \gamma/(R_p + R_o)$, where R_p is the curvature radius in the perpendicular cross section to droplet-liquid metal interface at this point, and R_o is the curvature radius of the orthogonal cross section to R_p . R_p is determined by the contact angle and the capillary length of the droplet. In the cases of small and large droplets, the contact angle and capillary length are the same. Thus, R_p is the same in both cases. In the orthogonal cross section, the projection of R_o on the droplet-liquid metal interface equals to the droplet radius, i.e., $R_{os} = R_s/\sin \theta_e$ for small droplet and $R_{ol} = R_l/\sin \theta_e$ for large droplet, respectively. θ_e is the equilibrium contact angle of a droplet on the surface of liquid metal. According to the Laplace equation, the small droplet has a stronger resilience, i.e., $\gamma/(R_p + R_s/\sin \theta_e) > \gamma/(R_p + R_l/\sin \theta_e)$. Thus, the small

droplet has a stronger inhibition on the fluctuation of the contact line. It tends to have a smaller perturbation than the larger droplet.

For a rotating droplet, the deformation of the droplet is dominated by a force balance between the surface tension, constant pressure, and centrifugal force according to the analysis of Brown and Scriven.⁴¹ The relationship is expressed as

$$2H\gamma = \Delta p_0 + \Omega^2 R \Delta \rho, \quad (1)$$

where $H = \text{div} \mathbf{n}$ is the local mean curvature of the droplet surface, \mathbf{n} is the unit normal vector to the surface, γ is the surface tension, $\Delta \rho$ is the density difference between the droplet and the surrounding fluid, Ω is the angular velocity of the droplet, R is the radius of the rotating droplet, and Δp_0 is the pressure difference across the droplet surface at the axis of rotation. m is calculated as $m = 2\pi/4\psi$, where ψ is the circumferential angle corresponding to a quarter wavelength [Fig. 4(d)]. We could assume a case in which the boundary propagates outward in the form of an arc, experiences a nonequilibrium B_1 stage, and keeps a force balance at the B_2 stage. At B_2 , the local curved boundary is tangential to the overall droplet radius R_w , i.e., the radius of the local curved boundary R_b is perpendicular to R_w . Thus, we have the relation $\tan \psi = R_b/R_w$, i.e., $\psi = \arctan(R_b/R_w)$. The force balance at this stage is $\gamma/R_b = \xi$, where $\xi = \Delta p_0 + \rho \Omega^2 R_w$. The local radius R_b can be

written as $R_b = \gamma/\xi$. Then, substituting the formula for ψ and R_b into that for m , we can get

$$m = \frac{\pi}{2} \left(\arctan \frac{\gamma}{\xi R_w} \right)^{-1}. \quad (2)$$

There is a relationship between the volume V of the droplet and the droplet radius R_w , i.e., $V = \pi R_w^2 h$. h is the thickness of the droplet as the acid droplet shows a pancake shape on the surface of liquid metal. It is related to the capillary length and the equilibrium contact angle. The capillary length is expressed as $k^{-1} = (\gamma_{lv}/\rho g)^{1/2}$, where γ_{lv} is the liquid-vapor interface tension, ρ is the density of the liquid, and g is the gravitational acceleration. The droplet surface can be regarded as the combination of a flat part in the bulk and a curved part in the boundary of the droplet. The thickness of the droplet can be recast in terms of the capillary length $h = 2k^{-1} \sin(\theta_e/2)$, where θ_e is the equilibrium contact angle. Thus, the droplet radius R_w can be expressed with the volume of droplet V as $R_w = (V/\pi h)^{1/2}$,

$$m = \frac{\pi}{2} \left(\arctan \frac{\gamma(\pi h)^{1/2}}{\xi V^{1/2}} \right)^{-1}. \quad (3)$$

Figure 4(e) shows the comparison of the proposed model and experimental data on the relationship between m and V . The dots are obtained from experimental results, and the dotted line is the theoretical fitting with the model. For relatively large values of droplet volume, the droplet lobe number m decreases with the volume V , which is constant with the experimental results. When the droplet volume tends to be infinitely small, the repression of the droplet surface tension on the droplet surface oscillation will tend to infinity, which results in the reduction of the lobe number m of the droplet as shown in the fitting curve.

From the above experimental results and discussion, it is seen that Ω is inversely proportional to R . A simple model is employed to explain this phenomenon. The rotation originates from the boundary oscillation of the droplet. The change in energy is related to the droplet perimeter. When the droplet radius changes from R_0 to R (assuming $R = \alpha R_0$, the subscript “0” represents the initial state of the droplet), the energy variation related to the droplet rotation changes to $\alpha \Delta E$ from ΔE . The energy variation ΔE can be expressed as

$$\Delta E = \frac{1}{2} \int_0^{2\pi} \int_0^R \rho h d\vartheta dR v^2 = \frac{\rho h}{2} \int_0^{2\pi} d\vartheta \int_0^R \Omega^2 R^2 dR = \frac{\pi \rho h}{3} \Omega^2 R^3, \quad (4)$$

where ρ is the density of droplet; h is the constant thickness of the droplet, which is related to the capillary length since the droplet has a pancake shape with a constant thickness on liquid metal. ϑ and R represent the two polar coordinates. v is the velocity of the liquid unit. Thus, the energy variations corresponding to the initial case R_0 and the current case R are $\Delta E = \pi \rho h \Omega_0^2 R_0^3/3$ and $\alpha \Delta E = \pi \rho h \Omega^2 (\alpha R_0)^3/3$, respectively. Thus, we get $\alpha \Omega = \Omega_0$, or alternatively, $\Omega/\Omega_0 = 1/\alpha = R_0/R$. Thus, Ω is inversely proportional to R . The experimental results shown in Fig. 5(a) exhibit a linear relationship between R and Ω , which validates this analysis.

From the theory of Brown and Scriven and subsequent work,^{17,41,42} the deformation of a rotating droplet can be characterized by the dimensionless angular velocity $\Omega' = \sqrt{\rho \Omega^2 R^3/8\gamma}$. When Ω' reaches 0.56, a two-lobed “peanut” shape is observed. As Ω' reaches 0.71 and 0.75, the three- and four-lobed family branches out from the axisymmetric shapes. For a volume-controlled rotating droplet, the rotation lobe distribution is approximately consistent with that from classical theory. Multi-lobed shapes occur within the following ranges: two-lobed $\Omega' \sim 0.52$ to $\Omega' \sim 0.68$, three-lobed $\Omega' \sim 0.71$ to $\Omega' \sim 0.76$, and four-lobed $\Omega' \sim 0.74$ to $\Omega' \sim 0.79$ [Fig. 5(b)]. The distribution of multi-lobed shapes according to the plot of R and Ω' is shown in Fig. 5(c). The dots from the experimental data agree with the theory curve.

In summary, we have studied the multi-lobed shapes of rotating droplets based on IRCRD in this work. The deformation of rotating droplets is of great significance in fluids mechanics, nucleonics, and astrophysics. By controlling the volume, a droplet can develop four-, three-, and two-lobed shapes. This method differs from the previous ways of realizing the multi-lobed rotation of droplets by controlling the angular velocity with the assistance of external devices. A simple model has been proposed to explain the relationship between the droplet lobe number n and the droplet radius R . In addition, the dimensionless angular velocities Ω' have been analyzed. The relationships between n , R , and Ω' agree well with the theory of Scriven and Brown. This research offers a new method based on IRCRD that employs volume instead of angular velocity to study the deformation and fission of a rotating droplet and provides a new way to design devices including micro/nanomotors, soft pumps, and foldable devices.

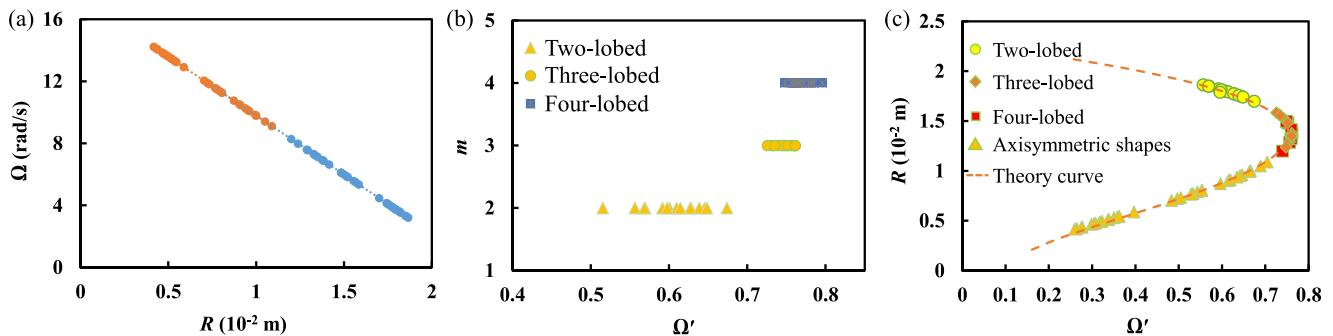


FIG. 5. (a) The variation of Ω with R shows a linear relationship between the two, which is consistent with theoretical analysis. (b) The distribution of the lobe numbers n corresponding to dimensionless angular velocities Ω' . (c) The relationship between R and Ω' . The dots are experimental measurements and the dotted line represents the theory curve.

See the [supplementary material](#) for details of the case in which a two-lobed droplet splits into two individual droplets with the continuous injection of liquid.

We thank Professor Ya-Pu Zhao for fruitful discussions. This work was supported by the National Natural Science Foundation of China (No. 12202461), the China Postdoctoral Science Foundation (No. 2022M710157), and the Outstanding Youth Science Foundation of Shenzhen Institutes of Advanced Technology, Chinese Academy of Sciences (No. E25420).

AUTHOR DECLARATIONS

Conflict of Interest

The authors have no conflicts to disclose.

Author Contributions

Zhan-Long Wang: Conceptualization (lead); Data curation (equal); Formal analysis (equal); Funding acquisition (equal); Investigation (equal); Methodology (equal); Project administration (equal); Resources (equal); Software (equal); Supervision (equal); Validation (equal); Visualization (equal); Writing – original draft (equal); Writing – review & editing (equal). **Kui Lin:** Conceptualization (supporting); Data curation (equal); Formal analysis (equal); Investigation (equal); Project administration (equal); Supervision (equal); Validation (equal); Visualization (equal); Writing – original draft (equal); Writing – review & editing (equal).

DATA AVAILABILITY

The data that support the findings of this study are available from the corresponding authors upon reasonable request.

REFERENCES

- S. Michelin, “Self-propulsion of chemically active droplets,” *Annu. Rev. Fluid Mech.* **55**, 77–101 (2023).
- L. Dong and Y. V. Kartashov, “Rotating multidimensional quantum droplets,” *Phys. Rev. Lett.* **126**, 244101 (2021).
- S. L. Butler, “Equilibrium shapes of two-phase rotating fluid drops with surface tension,” *Phys. Fluids* **32**, 012115 (2020).
- S. L. Butler, “Equilibrium shapes of two- and three-dimensional two-phase rotating fluid drops with surface tension: Effects of inner drop displacement,” *Phys. Fluids* **34**, 112103 (2022).
- M. Pi, F. Ancilotto, and M. Barranco, “Rotating ^3He droplets,” *J. Chem. Phys.* **152**, 184111 (2020).
- S. M. O. O’Connell, R. M. P. Tanyag, D. Verma *et al.*, “Angular momentum in rotating superfluid droplets,” *Phys. Rev. Lett.* **124**, 215301 (2020).
- B. Langbehn, K. Sander, Y. Ovcharenko *et al.*, “Three-dimensional shapes of spinning helium nanodroplets,” *Phys. Rev. Lett.* **121**, 255301 (2018).
- S. Tsuzuki, “Reproduction of vortex lattices in the simulations of rotating liquid helium-4 by numerically solving the two-fluid model using smoothed-particle hydrodynamics incorporating vortex dynamics,” *Phys. Fluids* **33**, 087117 (2021).
- V. Cardoso, O. J. C. Dias, and L. Gualtieri, “The return of the membrane paradigm? Black holes and strings in the water tap,” *Int. J. Mod. Phys. D* **17**, 505–511 (2008).
- B. V. Hokmabad, A. Nishide, P. Ramesh *et al.*, “Spontaneously rotating clusters of active droplets,” *Soft Matter* **18**, 2731–2741 (2022).
- L. N. Carenza, G. Gonnella, D. Marenduzzo *et al.*, “Rotation and propulsion in 3D active chiral droplets,” *Proc. Natl. Acad. Sci. U. S. A.* **116**, 22065–22070 (2019).
- A. F. Plateau, “Experimental and theoretical researches on figures of equilibrium of a liquid mass withdrawn from action of gravity,” *Trans. in. Ann. Rep. Smithsonian Inst.* **207** (1863).
- R. Tagg, L. Cammack, A. Croonquist *et al.*, “Rotating liquid drops: Plateau’s experiment revisited,” Jet Propulsion Laboratory, California Institute of Technology Pasadena, Report No. 80-66 (JPL Publication, 1980).
- A. Carbonaro, L. Cipelletti, and D. Truzzolillo, “Spinning drop dynamics in miscible and immiscible environments,” *Langmuir* **35**, 11330–11339 (2019).
- Z. Jiang, Y. Gan, and Y. Luo, “Effect of viscosity ratio on the dynamic response of droplet deformation under a steady electric field,” *Phys. Fluids* **32**, 053301 (2020).
- T. G. Wang, *Advances in Applied Mechanics*, edited by J. W. Hutchinson and T. Y. Wu (Elsevier/Academic Press, 1988), Vol. 26.
- R. J. A. Hill and L. Eaves, “Nonaxisymmetric shapes of a magnetically levitated and spinning water droplet,” *Phys. Rev. Lett.* **101**, 234501 (2008).
- L. Liao and R. J. A. Hill, “Shapes and fission of highly charged and rapidly rotating levitated liquid drops,” *Phys. Rev. Lett.* **119**, 114501 (2017).
- K. A. Baldwin, S. L. Butler, and R. J. Hill, “Artificial tektites: An experimental technique for capturing the shapes of spinning drops,” *Sci. Rep.* **5**, 7660 (2015).
- Y. Gu, C. Chen, Z. Mao *et al.*, “Acoustofluidic centrifuge for nanoparticle enrichment and separation,” *Sci. Adv.* **7**, eabc0467 (2021).
- C. L. Shen, W. J. Xie, and B. Wei, “Parametrically excited sectorial oscillation of liquid drops floating in ultrasound,” *Phys. Rev. E* **81**, 046305 (2010).
- P. C. Lin and L. I., “Acoustically levitated dancing drops: Self-excited oscillation to chaotic shedding,” *Phys. Rev. E* **93**, 021101 (2016).
- D. Boniface, J. Sebilliau, J. Magnaudet *et al.*, “Spontaneous spinning of a dichloromethane drop on an aqueous surfactant solution,” *J. Colloid Interface Sci.* **625**, 990–1001 (2022).
- V. Pimienta and C. Antoine, “Self-propulsion on liquid surfaces,” *Curr. Opin. Colloid* **19**, 290–299 (2014).
- A. Chakrabarti, G. P. T. Choi, and L. Mahadevan, “Self-excited motions of volatile drops on swellable sheets,” *Phys. Rev. Lett.* **124**, 258002 (2020).
- H. R. Vutukuri, M. Lisicki, E. Lauga *et al.*, “Light-switchable propulsion of active particles with reversible interactions,” *Nat. Commun.* **11**, 2628 (2020).
- P. Liu, H. Zhu, Y. Zeng *et al.*, “Oscillating collective motion of active rotors in confinement,” *Proc. Natl. Acad. Sci. U. S. A.* **117**, 11901–11907 (2020).
- J. Ignes-Mullol, G. Poy, and P. Oswald, “Continuous rotation of achiral nematic liquid crystal droplets driven by heat flux,” *Phys. Rev. Lett.* **117**, 057801 (2016).
- R. Zhang, A. Mozaffari, and J. J. de Pablo, “Autonomous materials systems from active liquid crystals,” *Nat. Rev. Mater.* **6**, 437–453 (2021).
- Z. Wang, X. Wang, Q. Miao *et al.*, “Realization of self-rotating droplets based on liquid metal,” *Adv. Mater. Interfaces* **8**, 2001756 (2021).
- Z. Wang, X. Wang, Q. Miao *et al.*, “Spontaneous motion and rotation of acid droplets on the surface of a liquid metal,” *Langmuir* **37**, 4370–4379 (2021).
- V. Cardoso and O. J. Dias, “Rayleigh-Plateau and Gregory-Laflamme instabilities of black strings,” *Phys. Rev. Lett.* **96**, 181601 (2006).
- V. Cardoso and L. Gualtieri, “Equilibrium configurations of fluids and their stability in higher dimensions,” *Classical Quantum Gravity* **23**, 7151–7198 (2006).
- S. Bhattacharyya, V. E. Hubeny, R. Loganayagam *et al.*, “Local fluid dynamical entropy from gravity,” *J. High Energy Phys.* **06**, 055 (2008).
- F. P. Riley, P. M. McMackin, J. M. Lopez *et al.*, “Flow in a ring-sheared drop: Drop deformation,” *Phys. Fluids* **33**, 042117 (2021).
- Z. Wang, K. Lin, and Y.-P. Zhao, “The effect of sharp solid edges on the droplet wettability,” *J. Colloid Interface Sci.* **552**, 563–571 (2019).
- K. Nagai, Y. Sumino, H. Kitahata *et al.*, “Mode selection in the spontaneous motion of an alcohol droplet,” *Phys. Rev. E* **71**, 065301 (2005).
- P. G. de Gennes, “On fluid/wall slippage,” *Langmuir* **18**, 3413–3414 (2002).
- S. Granick, Y. Zhu, and H. Lee, “Slippery questions about complex fluids flowing past solids,” *Nat. Mater.* **2**, 221–227 (2003).
- J. L. Liu and R. Xia, “A unified analysis of a micro-beam, droplet and CNT ring adhered on a substrate: Calculation of variation with movable boundaries,” *Acta Mech. Sin.* **29**, 62–72 (2013).
- R. A. Brown and L. E. Scriven, “The shape and stability of rotating liquid drops,” *Proc. R. Soc. London, Ser. A* **371**, 331–357 (1980).
- P. Aussillous and D. Quéré, “Shapes of rolling liquid drops,” *J. Fluid Mech.* **512**, 133–151 (2004).